# Microstructural Characterization and Hardness Properties of Plasma Sprayed Biomedical Coatings

MORKS Magdi F.* and KOBAYASHI Akira **


## Abstract

*Hydroxyapatite coatings were sprayed on 304 stainless steel substrates by using a gas tunnel type plasma system (GTTP). This system consists of two plasma sources: a gun which produces internal low power plasma (1.3-8 kW) and vortex which produces external high power plasma (10-40 kW). In this work, the arc gun current was changed while the vortex arc current was kept constant at 450 A. The effect of gun power on the microstructure and mechanical properties of HA coatings were investigated. Five gun currents were adjusted (0, 30, 50, 70 and 100 A) at the same vortex current (450 A) for sprayed HA coatings. The microstructure of resulting coatings was investigated by XRD and SEM. Hardness values of HA coatings sprayed at different arc gun currents were also investigated. The results showed that the gun currents affected the microstructure and porosity of HA coatings. Moreover, the hardness was slightly decreased as the gun current increased.*


**KEYWORDS**: (Hydroxyapatite), (Plasma spraying), (Gun current), (Microstructure), (Hardness)

## 1. Introduction

Hydroxyapatite material is extensively used as a biomedical material to improve the compatibility properties of metallic implants (Ti, Ti-alloy, stainless steel). This material can be deposited on the metallic implants and used in orthopaedic surgery to replace the broken bone. Pure HA materials can assist the build up of new tissue and fix the implants inside the body. Although many methods[1-5] have been used to deposit pure HA coatings, the current researches are interested to deposit HA coatings by using thermal spraying technologies because these methods have the ability of spraying thick HA coatings with good adhesion and low porosity in short times. These methods include HVOF, DGUN and conventional plasma spraying[6-8]. The problem associated with thermal spraying method is the decomposition of HA coatings during spraying to form oxyhydroxyapatite (OHA), tetracalcium phosphate (TTCP), α and/or β–tricalcium phosphate (α–TCP, β–TCP), amorphous phase and calcium oxide (CaO) materials[9-11]. The decomposition is related to the high temperature of thermal spraying flame. For that a careful control of thermal spraying parameters is required to prevent the decomposition and achieve high quality HA coatings. Many studies have been done to show the effect of plasma spraying parameters on the microstructure and mechanical properties of sprayed HA coatings[12-14].

Gas tunnel type plasma spraying (GTTP) developed in Osaka University[15-18] is a unique method to deposit high quality ceramics[19-21] due to its high power and high spraying efficiency. The GTTP system is composed of two sources of plasma: gun and vortex. It has two anodes and one cathode. The nozzle diameter of the vortex is 20mm and the gun nozzle diameter is 8 mm. The author has used this system to deposit HA coatings and studied the effect of spraying parameters such as spraying distances, plasma power and arc gas flow rate on the microstructure and mechanical properties of HA coatings[22-24]. It was found that these spraying parameters affect greatly the microstructure and mechanical properties of sprayed HA coatings.

In this study the vortex arc current was kept constant at 450 (A) and the gun current was varied from 0 – 100 A. The microstructure and mechanical properties of the resulting coatings will be investigated. It is expected that the change of gun current will affect the properties of the resulting HA coatings.

## 2. Experimental Procedure

### 2.1 Materials

Pure hydroxyapatite powder of spherical shape and particle size range of 10-45 μm was supplied by and used as spraying materials. The scanning electron micrograph and x-ray diffraction pattern of the HA powder are shown in Fig. 1. Substrate material is 304 stainless steel of dimensions 50 x 50 x 2.5 mm. The substrate was grit blasted by alumina powder to clean and roughen the surface before spraying (Ra 3-7 μm).

### 2.2 Spraying process

A systematic diagram of the gas tunnel type plasma

† Received on May 12, 2006
* Foreign Visiting Researcher
** Associate Professor

Transactions of JWRI is published by Joining and Welding Research Institute, Osaka University, Ibaraki, Osaka 567-0047, Japan

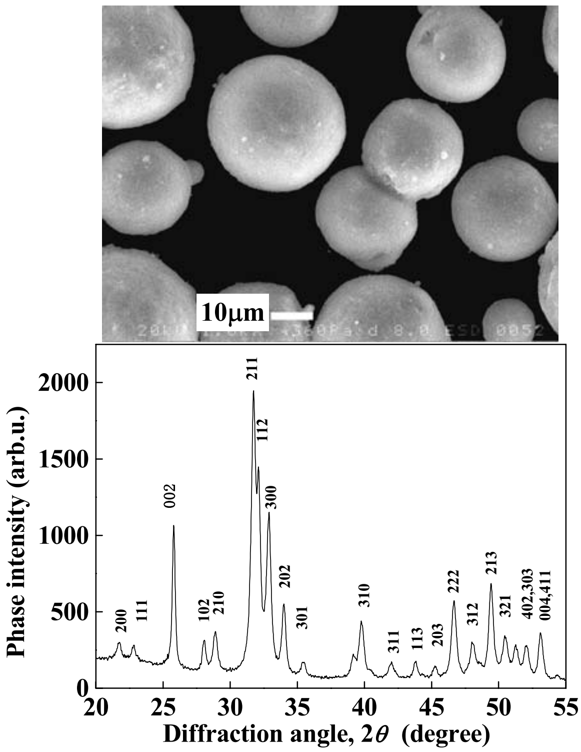


**Fig. 1** Morphology and X-ray diffraction pattern of starting HA powder.

**Table 1** Spraying parameters for HA coatings.

| | |
|---|---|
| Arc gun current (A) | 0-100 |
| Arc vortex current (A) | 450 |
| Working gas flow rate (l/min) | 120 |
| Carrier gas flow rate (l/min) | 5 |
| Powder size (μm) | +10-45 |
| Spraying distance (mm) | 60 |
| Substrate traverse speed (mm/s) | 40 |

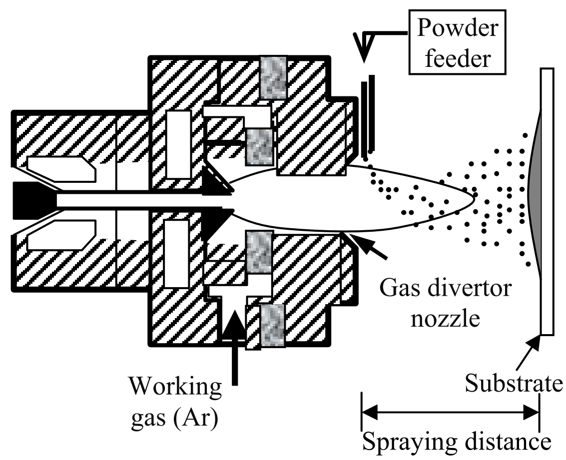


**Fig. 2** Schematic diagram of gas tunnel type plasma spraying torch.

spraying torch (GTTP) is shown in Fig.2. HA powder was externally fed as shown in the figure. The spraying conditions are listed in Table 1. The spraying system has two parts: gun and vortex. The vortex arc current was kept constant at 50 (A) and the gun arc current was changed from 0 to 100 (A). The arc gas (Ar) flow rate was kept constant at 120 l/min for all experiments. No secondary arc gas was used to avoid over heating of sprayed particles. The gun power and vortex power were calculated at different arc gun currents. The substrate was preheated by the plasma jet to approximately 600 K to allow good adhesive bonding between the first coating lamella and substrate.

### 2.3 Characterization techniques

Feedstock and coatings morphologies were examined by an ERA-8800FE scanning electron microscope. The examined cross-section samples were mounted in epoxy resin, polished and buffed with alumina paste (1.0, 0.3, and 0.05 μm, respectively) to get a mirror finished surface. All samples were coated with a thin film of gold using a gold ion sputtering device to make them electrically conductive before SEM examination.

Phase identification of feedstock and coatings were examined by a JEOL JDX-3530M X-ray diffractometer system with CuKα radiation source; the operating voltage was 40 kV and current 40 mA.

Hardness tests were performed on polished and buffed cross-section coated samples using Akashi AAV-500 series hardness tester. The load used was 490.3 mN and the load time was 20 s. Each hardness value is the average of 10 readings.

Porosity of HA coatings was evaluated by an image analyzing method using computerized optical microscope. The HA surface images were captured by the optical microscope and analyzed using image analyzing software which evaluate the pores area according to the color differences between the pores and coat.

## 3. Results and Discussion

### 3.1 Coating microstructure and phase structure

Scanning electron micrographs of HA coatings sprayed at different gun currents are shown in Fig. 3. It is clear from the figure that all coatings are porous and contain unmelted particles. However, the porosity and the number of unmelted particles decrease for sprayed coatings at 0, 70 and 100 A. The microstructure of HA coatings sprayed at 30 and 50 A of gun currents shows many pores and unmelted particles. From the morphologies of cross-sections of sprayed HA coatings, one can recognize that the gun current greatly affects the microstructure and coating porosity. For more details about the coatings morphology, the surface of sprayed HA coatings sprayed at different gun currents was observed as shown in Fig. 4. The morphologies of HA coatings surfaces show spherical unmelted particles in all coatings. However, HA coatings sprayed at 0 and 100 A (gun currents) have few unmelted particles and the coatings are mainly formed from the impact of fully

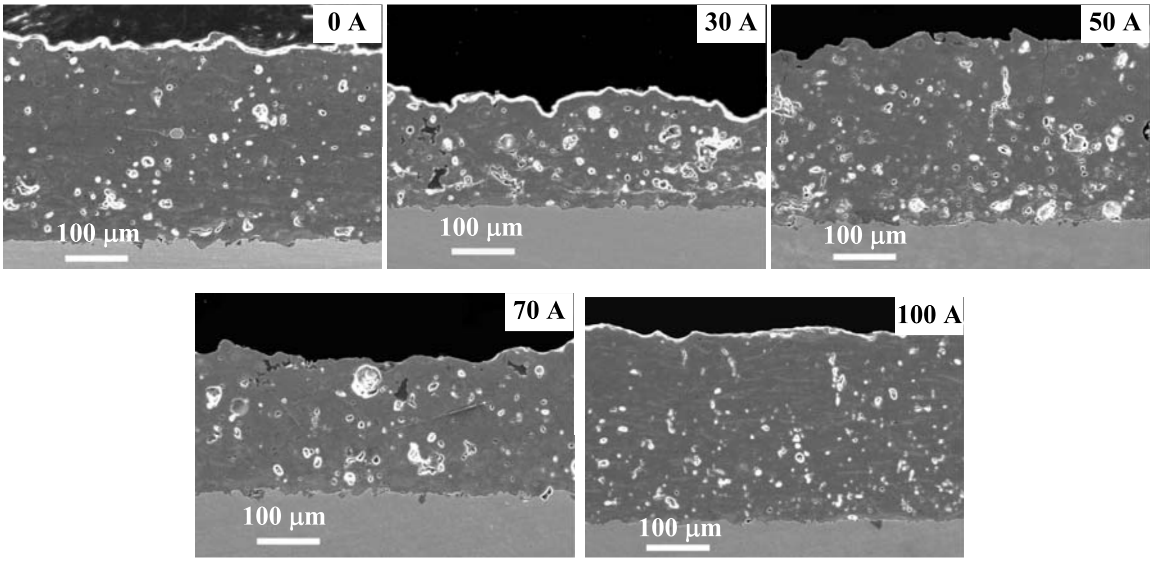


**Fig.3** SEM micrographs of HA coatings sprayed at different gun current.

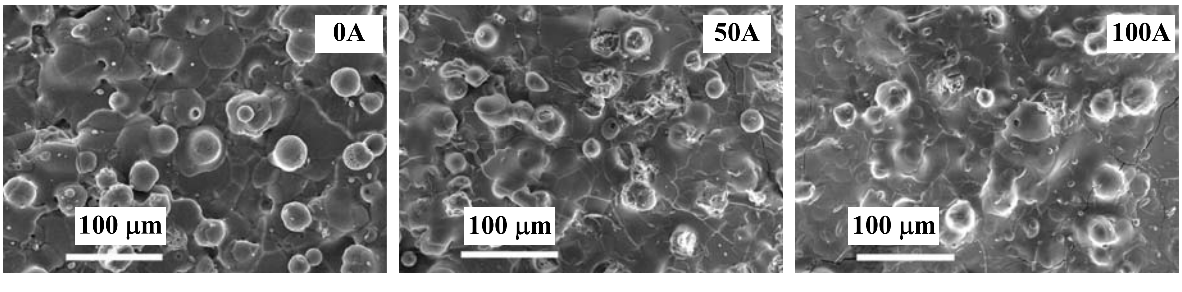


**Fig. 4** Surface morphologies of HA coatings sprayed at different gun currents.

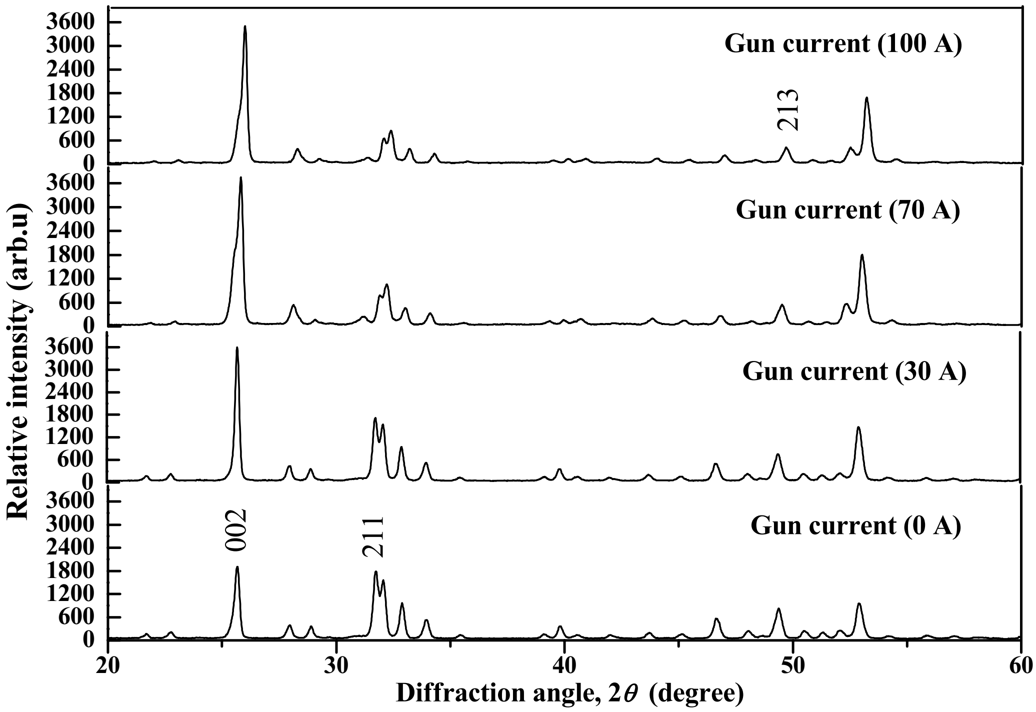


**Fig 5** X-ray diffraction patterns of HA coating sprayed at different gun currents.

melted or semi-melted particles. Moreover, the splats of HA coatings sprayed at 100 A of gun current seem to be more compact which indicate that the particle temperature may be higher than that sprayed at 0 A of gun current.

X-ray diffraction patterns of HA coatings sprayed at different gun currents are shown in Fig. 5. All the peaks of sprayed coatings belong to HA. There is no contamination by other phases such as Oxy-HA, tri-calcium phosphate, tetra-calcium phosphate or calcium dioxide. The XRD data indicate that there is no decomposition of HA coatings during spraying. Although the coatings are composed of HA, there are some differences in the peak intensities of the coatings sprayed at different arc gun currents. The intensities of the peak (002) increase as the gun current increases. On the other hand, the peak intensities of (211) decrease during spraying at high arc gun currents of 70 and 100 A. The differences of peak intensities are related to the change of phase crystallography of the HA coatings. The reason for change the phase crystallography of the material may be due to the difference in particle temperature during spraying or heat treatment of hot sprayed particles by the plasma jet.

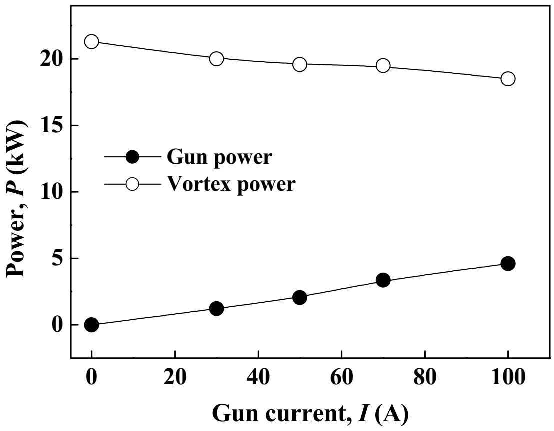


**Fig. 6** Vortex and gun power at different gun currents and 450 (A) vortex current.

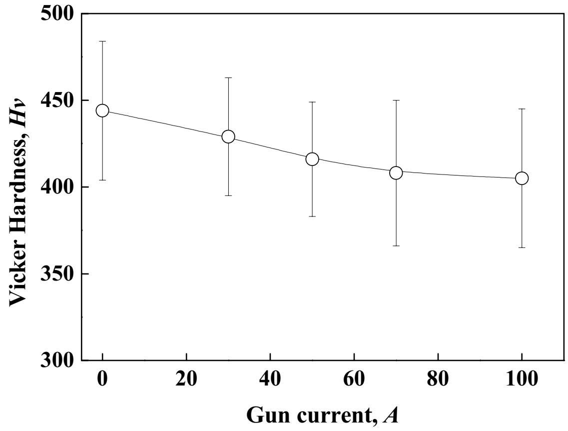


**Fig. 7** Hardness values of HA coatings sprayed at different arc gun currents and 450A vortex arc current.

The results of x-ray diffraction give some information about the effect of gun current on the particle temperature during spraying.

### 3.2 Vortex and gun power

The power of vortex and gun was measured at different arc gun current and at constant vortex current of 450 A as shown in Fig. 6. The purpose of this measurement is to know whether the arc gun current affects the vortex power or not. It is seen from the figure that the gun power increases to reach 4 kW as the arc gun current increases to 100 A. The gun power increases mainly due to the increase of arc gun currents. On the other hand, the vortex power value reaches maximum at gun current 0 A (gun power 0 kW) of value 21.3 kW. The voltage of vortex is 44.5 V in this case. However, at an arc gun current of 100 A the measured vortex power is 18.5 kW of voltage value of 41 V. The decrease of vortex power by increasing arc gun current may be related to the consumption within the gun of some working gas (Ar). The total amount of gas flow reaching the vortex decreases by increasing the gun power. The vortex power was decreased from 21.3 to 20 kW by increasing the arc current from 0 to 30 A. However, the vortex power decreased by 0.5 kW for every 20-30 (A) increase of gun current. The total power of the GTTP gun (vortex + gun) increases from 21.3 to 23 kW as the gun current increases from 0 to 100 A.

The HA powder was externally fed and only interacted with vortex plasma jet. In this case, the properties of HA coatings depend on the power and properties of vortex plasma jet. At a gun power of 0 kW, the vortex power value is maximum (21.3 KW) and the particle temperature increases and as a result dense and low porosity coatings are formed as illustrated in Fig 3 (0A). As the gun power increases the vortex power slightly decreases and as a result HA coatings with some pores and unmelted particles are formed as shown in Fig. 3 (30,50,70A). At high gun power (4.6 kW), the vortex power is lower (18.5 kW) mainly due to the decrease of the working gas flow (Ar) which is consumed by the gun to form the internal plasma jet. Although the vortex power was decreased, dense structure coatings were formed as shown in Fig. 3 (100 A). There are two reasons: the first is that particle velocity was decreased as the vortex power was decreased and as a result the particle temperature increases due to the increase of particle dwell time in the plasma jet. The second reason is that the heat energy of the plasma formed by the gun (4.6 kW) transfers and increases the energy of the plasma formed by the vortex.

### 3.3 Hardness

Hardness values of HA coatings sprayed at different gun currents was measured on the cross-sections of polished and buffed samples as shown in Fig. 7. The results show that the hardness values slightly decreases as the gun currents increases. The main value of hardness decreases from *Hv* 440 for sprayed coating at 0 A of gun current to *Hv* 406 for sprayed coating at 100 A of gun current. From the x-ray diffraction pattern, there was a change in phase intensities of HA coatings as the gun current increases. The presence of pores and unmelted particles decreases the hardness mainly due to the weakness of cohesion bonds due to the presence of pores.

## 4. Conclusions

Arc gun current affects the vortex power of the gas tunnel type plasma spraying. The microstructure and mechanical properties of the HA coatings were also affected. The results can be summarized as follow:

(1) At 0 and 100 (A) of gun current a dense with low porosity HA coatings were formed mainly due to the high vortex power (21.3 kW- 0 kW/ gun power) and the effect of gun power (4kW) on the vortex power at high gun current (100 A).

(2) The hardness value of sprayed HA coatings was slightly decreased as the gun current increases due to the decrease of vortex power and the formation of pores and unmelted particles.

**Acknowledgment**

This work was financially supported by Japan Society for the Promotion of Science (JSPS) of Grant-on-Aid No. 17.05 102. The authors would like to gratefully acknowledge Smart Processing Research Center for provision the plasma system and characterization devices.

**References**

1) V.W. Raemdonck, P. Ducheyne, D.P. Meester, J. Am. Ceram. Sot. 67 (1984) 381-384.
2) K. Yamashita, T. Arashi, K. Kitagaki, S. Yamada, T. Umegaki, K.J. Ogawa, Preparation of apatite thin films through rf-sputtering from calcium phosphate glasses, Am. Ceram. Sot. 77 (1994) 2401-2407.
3) C.S. Kim, P. Ducheyne, Compositional variations in the surface and interface of calcium phosphate ceramic coatings on Ti and Ti-6Al-4V due to sintering and immersion, Biomaterials 12 (1991) 461-469.
4) X. Nie, A. Leyland, A. Matthews, Deposition of layered bioceramic hydroxyapatite/$TiO_2$ coatings on titanium alloys using a hybrid technique of micro-arc oxidation and electrophoresis, Surf. Coat. Technology 125 (2000) 407-414.
5) M. Shirkhanzadeh, Bioactive calcium phosphate coatings prepared by electrodeposition, J. Mater. Sci. Lett 10 (1991) 1415-1417.
6) H.C. Gledhill, I.G. Turner, C. Doyle, Direct morphological comparison of vacuum plasma sprayed and detonation gun sprayed hydroxyapatite coatings for orthopaedic applications, Biomaterials 20 (1999) 315-322.
7) P.L. Silva, J.D. Santos, F.J. Monteiro, J.C. Knowles, Adhesion and microstructural characterization of plasma-sprayed hydroxyapatite/glass ceramic coatings onto Ti-6A1-4V substrates, Surface and Coatings Technology I02 (1998) 191-196.
8) R.S. Lima, K.A. Khor, H. Li, P. Cheang, B.R. Marple, HVOF spraying of nanostructured hydroxyapatite for biomedical applications, Materials Science and Engineering A 396 (2005) 181-187.
9) R. Mc Pherson, N. Gane, T.J. Bastow, J. Mater. Sci. Mater. Med. 6 (1995) 327.
10) K.A. Gross, C.C. Berndt, J. Biomed. Mater. Res. 39 (1998) 580.
11) K.A. Gross, C.C. Berndt, H. Herman, J. Biomed. Mater. Res. 39 (1998) 407.
12) P.L. Silva, J.D. Santos, F.J. Monteiro , J.C Knowles, Adhesion and microstructural characterization of plasma-sprayed hydroxyapatite/glass ceramic coatings onto Ti-6A1-4V substrates, Surf. Coat. Technolo I02 (1998) 191-196
13) C.H. Quek, K.A. Khor, P. Cheang, Influence of processing parameters in the plasma spraying of hydroxyapatite/Ti-6A-4V composite coatings, Journal of Materials Processing Technology 89-90 (1999) 550-555
14) S. Dyshlovenko, L. Pawlowski, P. Roussel, D. Murano, A. Le Maguer, Relationship between plasma spray operational parameters and microstructure of hydroxyapatite coatings and powder particles sprayed into water, Surface & Coatings Technology 200 (2006) 3845– 3855
15) A. Kobayashi, Y. Arata, and Y. Habara, *J. High Tem. Soc*. Vol 13 (3) (1987) pp 116-124.
16) Y. Arata and A. Kobayashi, *J. Appl. Phys*. 59 (9) (1986) pp 3038-3044.
17) A. Kobayashi, *Weld. International*, Vol 4 (4) (1990) pp 276-282.
18) Y. Arata, A. Kobayashi and Y. Habara, *J. Appl. Phys*. Vol 62 (12) (1987) pp 4884-4889
19) S.Sharafat , A.Kobayashi, Y.Chen , N.M. Ghoniem, Plasma spraying of micro-composite thermal barrier coatings, Vacuum 65 (2002) 415–425.
20) A. Kobayashi, T. Kitamura, Effect of heat treatment on high-hardness zirconia coatings formed by gas tunnel type plasma spraying, Vacuum 59 (2000) 194}202.
21) N.F. Fahim and A. Kobayashi, Gas tunnel type plasma spraying deposition and microstructure characterization of silicon carbide films for thermoelectric applications, *Materials Letters, **In Press.***
22) M. F. Morks, Akira Kobayashi, Gas Tunnel Type Plasma Spraying of Hydroxyapatite Coatings" in Proc. of The International Thermal Spray Conference, ITSC May 15-18 2006, Seattle, Washington/USA.
23) M. F. Morks, Akira Kobayashi, "Microstructure and Mechanical Properties of Hydroxyapatite Coatings Prepared by Gas Tunnel Type Plasma Spraying" International Symposium on Smart Processing Technology, ISMPT 14-15 Nov. 2005, Osaka, Japan.
24) M. F. Morks, Akira Kobayashi **"**Influence of Spray Parameters on the Features of Gas Tunnel Type Plasma Sprayed Hydroxyapatite Coatings" Trans. JWRI, Vol. 34, (2005), No.2.